The Journal of Experimental Biology 212, 3026-3034
Published by The Company of Biologists 2009
doi:10.1242/jeb.030064

The adhesive delivery system of viscous capture threads spun by orb-weaving spiders

Brent D. Opell* and Mary L. Hendricks
Department of Biological Sciences, Virginia Polytechnic Institute and State University, Blacksburg, VA 24061, USA
*Author for correspondence (bopell@vt.edu)

Accepted 11 June 2009

SUMMARY

The sticky viscous capture threads in araneoid orb-webs are responsible for retaining insects that strike these webs. We used features of 16 species' threads and the stickiness that they expressed on contact plates of four widths to model their adhesive delivery systems. Our results confirm that droplets at the edges of thread contact contribute the greatest adhesion, with each successively interior droplet contributing only 0.70 as much adhesion. Thus, regardless of the size and spacing of a thread's large primary droplets, little adhesion accrues beyond a span of 20 droplets. From this pattern we computed effective droplet number (EDN), an index that describes the total droplet equivalents that contribute to the stickiness of thread spans. EDN makes the greatest positive contribution to thread stickiness, followed by an index of the shape and size of primary droplets, and the volume of small secondary droplets. The proportion of water in droplets makes the single greatest negative contribution to thread stickiness, followed by a thread's extensibility, and the area of flattened droplets. Although highly significant, this six-variable model failed to convincingly describe the stickiness of six species, a problem resolved when species were assigned to three groups and a separate model was constructed for each. These models place different weights on the variables and, in some cases, reverse or exclude the contribution of a variable. Differences in threads may adapt them to particular habitats, web architectures or prey types, or they may be shaped by a species' phylogeny or metabolic capabilities.

Key words: adhesive system, capture thread, orb-web, prey capture, viscous thread.

INTRODUCTION

Capture thread is the sticky, spiral component of a spider's orb-web that is supported by the web's non-sticky radial lines. By lengthening prey retention time, these sticky threads give a spider more time to locate, run to and subdue prey before they escape from the web (Chacón and Eberhard, 1980), a capability that is particularly important for the capture of large, profitable prey (Blackledge and Eliason, 2007). Two sub-clades of orb-weaving spiders comprise the Araneoidea clade, the Deinopoidea and the Araneoidea (Coddington and Levi, 1991; Griswold et al., 1998; Griswold et al., 2005). Like their non-orb-weaving ancestors, the Deinopoidea produce dry, cribellar capture threads formed of thousands of fine protein fibrils that are supported by a pair of axial lines (Eberhard and Pereira, 1993; Opell, 1994; Opell, 1999; Peters, 1984; Peters, 1986; Peters, 1992). In contrast, the orb-weaving members of the more diverse Araneoidea produce viscous capture threads composed of regularly spaced aqueous droplets supported by a pair of axial fibrils (Peters, 1986; Tillinghast et al., 1993; Vollrath, 1992; Vollrath et al., 1990; Vollrath and Tillinghast, 1991). At the center of each droplet is a glycoprotein granule that is thought to confer thread stickiness (Tillinghast et al., 1993; Vollrath and Tillinghast, 1991). The fluid that covers these granules and surrounds the axial fibers contains hydrophilic compounds, which attract atmospheric moisture, maintaining the droplet volume (Townley et al., 1991; Vollrath et al., 1990).

Each of a spider's paired median spinnerets bears a single flagelliform gland spigot and two aggregate gland spigots. The flagelliform glands produce axial fibers and the aggregate glands produce viscous aqueous material. Aggregate gland material initially forms a continuous cylinder around the fibers, but quickly condenses into a series of regularly spaced droplets. In some species these droplets have a pattern of larger primary droplets with smaller secondary droplets between them (Fig. 1).

Just as a thread's axial fibers and viscous droplets are physically linked, so too are they functionally linked (Agnarsson and Blackledge, 2009). Thread adhesion is generated when droplets contact a surface and, as the thread is pulled from this surface, the adhesion of multiple droplets is recruited by the axial fibers in what has been termed a suspension bridge mechanism (Opell and Hendricks, 2007). This is demonstrated by the observation that when the stickiness of viscous threads is measured with contact plates of increasing width, thread stickiness increases, something that is not observed when this procedure is used to measure the stickiness of cribellar threads (Opell and Schwend, 2008a). This mechanism operates imperfectly, with each successive pair of droplets interior to the edge of thread contact contributing progressively less adhesion until a limiting number of droplets contacts a surface, after which no additional thread stickiness is achieved (Opell and Hendricks, 2007). The contribution of axial fiber extensibility can be documented by stretching threads to reduce their extensibility and then measuring their stickiness with contact plates whose widths are increased in proportion to thread elongation, thereby maintaining the number of droplets that contribute to a thread's stickiness (Opell et al., 2008). This procedure shows that the per droplet stickiness of stretched threads is less than that of threads at their native tensions and indicates that axial fiber extensibility accounts for roughly one-third of a viscous thread's stickiness.

In this study we confirm the hypotheses supported by these earlier studies and examine other features that affect the stickiness of viscous threads by studying threads produced by 16 araneoid species

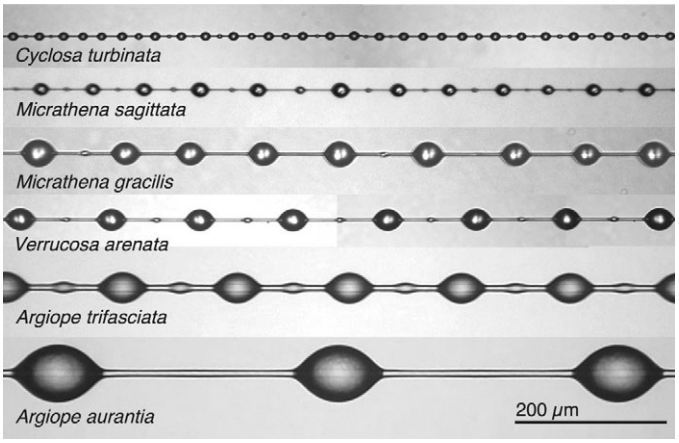

Fig. 1. Viscous threads of some of the species that were studied.

from three families. We include viscous threads with a wide range of droplet sizes and spacing (Fig. 1; Table 1). We measure the stickiness of each species' threads with contact plates of four widths and determine the size, shape, spacing and water content of their droplets. We also characterize the residual extensibility of their axial fibers. The six-variable model that we develop accounts for the contributions of the thread's larger primary droplets and of its smaller secondary droplets and explains 88% of the variance observed in these 64 mean stickiness values. Dividing these species into three groups, whose models weigh the contributions of variables differently, explains over 96% of the variance and shows that there are different pathways to achieving thread adhesion.

MATERIALS AND METHODS

Species studied and thread collection

We collected threads from newly spun orb-webs constructed by adult females of 16 Araneoidea species: one species from the family Theridiosomatidae: *Theridiosoma gemmosum* (L. Koch); three species from the family Tetragnathidae: *Meta ovalis* (Gertsch), *Leucauge venusta* (Walckenaer) and *Tetragnatha elongata* Walckenaer; and 12 from the family Araneidae: *Micrathena gracilis* (Walckenaer), *Micrathena sagittata* (Walckenaer), *Argiope aurantia* Lucus, *Argiope trifasciata* (Forskål), *Metepeira labyrinthea* (Hentz), *Larinioides cornutus* (Clerck), *Cyclosa turbinata* (Walckenaer), *Verrucosa arenata* (Walckenaer), *Araneus pegnia* (Walckenaer), *Araneus bicentenarius* (McCook), *Araneus marmoreus* Clerck and *Mangora maculata* (Keyserling). Threads of *Meta ovalis* and *Araneus bicentenarius* were collected from forests at the base of Grandfather Mountain, Avery County, NC, USA. Threads of the other species were collected from sites within 10 km of Blacksburg, Montgomery County, VA, USA.

We collected threads on samplers made by gluing 4.8 mm wide brass bars at 4.8 mm intervals to microscope slides. Double-sided Scotch® tape (Tape 665; 3M, St Paul, MN, USA) on the bars held thread strands securely at their native tension. To ensure that physical and performance characteristics of an individual spider's threads were not affected by changes in environmental conditions, we photographed its threads and measured stickiness under the same laboratory temperature and per cent relative humidity (RH). Threads of all species except *Meta ovalis* and *Araneus bicentenarius* were photographed and tested for stickiness on the same day they were collected. Threads of these two species were processed 2–4 days after being collected. During this time these threads were kept either on microscope slide samplers or on the 15 cm diameter rings used to collect orb-web sectors. Threads were secured to the 5 mm wide rims and 5 mm wide central supporting bar of these rings by double-sided tape. Samplers were kept in closed microscope slide boxes and rings in tightly sealing plastic food storage boxes. These storage conditions combined with the high summer humidity probably maintained threads in a environment in which RH was above 50% while they were being transported to the laboratory, where they were then stored at 49% RH before being photographed and measured. This short delay in measuring threads that are protected from dust and other damage appears to have little effect on their droplet volumes and thread stickiness (Opell and Schwend, 2008b). However, as another study has shown that the axial fibers of viscous threads became stiffer and lost extensibility and strength when

Table 1. Features of viscous threads and the conditions under which they were measured

Species	*N*	Spider mass (mg)	Primary droplets per mm	Primary droplets		Secondary droplets		Temperature (°C)	Relative humidity
				Length (μm)	Width (μm)	Length (μm)	Width (μm)		
Argiope aurantia	5	841.9±138.7	3.5±0.4	62.7±3.2	40.2±6.3	20.9±2.3	10.2±1.3	23.7±0.1	48.6±0.3
Araneus marmoreus	10	498.5±74.2	3.7±0.3	67.1±4.5	50.2±3.6	26.4±2.5 (7)	15.9±1.7 (7)	24.1±0.4	51.5±2.1
Argiope trifasciata	11	510.8±82.0	6.1±0.6	41.5±2.5	25.1±1.8	22.5±2.0	10.8±0.9	22.5±0.2	39.1±3.4
Araneus bicentenarius	6	407.0±67.6	6.2±1.7	50.5±5.1	41.5±4.7	21.5±3.4	13.4±2.4	24.0±0.0	48.5±0.5
Larinioides cornutus	4	265.9±27.2	6.2±1.4	41.6±6.4	30.6±4.9	33.1±8.4	22.8±6.5	23.5±0.5	54.6±0.8
Verrucosa arenata	5	74.3±12.2	7.4±0.8	27.9±1.0	22.5±0.9	9.7±1.7 (4)	6.3±1.5 (4)	23.6±0.2	52.0±0.9
Araneus pegnia	9	65.7±7.1 (8)	8.6±0.7	38.6±3.6	28.3±2.4	16.2±5.7 (3)	10.0±4.0 (3)	23.3±0.2	53.8±0.4
Micrathena gracilis	5	73.4±9.5	9.9±1.9	30.2±2.2	23.5±1.8	14.3±1.5 (4)	8.2±1.0 (4)	23.6±0.2	51.6±1.2
Theridiosoma gemmosum	5	2.8±0.2 (4)	11.0±1.4	14.4±3.4	11.6±2.1	9.2±2.9	6.5±2.1	24.0±1.5	54.9±1.5
Micrathena sagittata	5	46.8±5.5	11.4±2.0	25.9±1.4	20.0±1.3	10.7±1.8	6.5±1.4	24.1±0.3	51.1±1.2
Tetragnatha elongata	4	71.0±17.2 (3)	13.0±1.4	28.2±4.8	20.0±3.1	10.3±0.6 (3)	4.9±1.3 (3)	26.0±0.0	54.6±0.1
Metepeira labyrinthea	8	10.4±1.0	17.5±3.5	23.5±1.9	16.4±1.4	9.3±1.3	5.4±1.0	23.5±0.2	53.1±0.5
Meta ovalis	8	19.3±2.2 (7)	20.6±2.4	14.9±0.9	11.9±0.9	5.2±0.6	3.5±0.5	23.6±0.2	49.6±0.5
Leucauge venusta	10	22.0±3.1	29.9±2.1	13.8±1.2	10.0±0.9	5.6±0.5 (7)	3.9±0.4 (7)	22.6±0.2	43.2±1.4
Cyclosa turbinata	9	7.2±0.8 (8)	33.4±6.9	13.2±1.0	9.8±0.8	7.0±0.3	4.9±0.2	22.6±0.2	32.1±5.0
Mangora maculata	6	11.2±1.0	67.6±9.0	4.4±0.3	4.5±0.2	3.0±0.2 (4)	3.2±0.2 (4)	23.6±0.2	50.6±0.5

Means ± 1 s.e. Numbers in parentheses give the sample size if less than that listed in the second column.

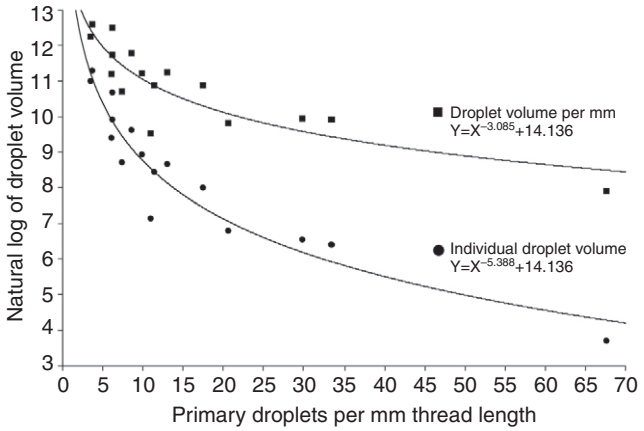

Fig. 2. Relationship between the number of primary droplets per millimeter thread length and the volume of individual droplets (lower) and primary droplet volume per millimeter (upper).

measured 20 days after they were spun (Agnarsson et al., 2008), it is not possible to completely rule out aging affects on thread stickiness.

Measuring droplet features

We made digital images of three suspended viscous threads from each spider's web at ×50 (for species with large droplets), ×125 (for species with smaller droplets) or ×250 magnification (for the species with tiny droplets) and of two threads at the next higher magnification. To simulate an insect adhering to the droplets, we then placed a glass cover slip across the brass supports on the microscope slide sampler to flatten thread droplets and made images of two threads at the higher magnification. We used ImageJ (ImageJ, 2006; http://www.uhnresearch.ca/facilities/wcif/imagej/) to measure these images.

The threads of many species feature large droplets with one or more smaller droplets between each pair of larger droplets (Fig. 1). We refer to larger droplets as primary droplets and smaller droplets as secondary droplets. To obtain the number of primary droplets per milllimeter (DPMM) we measured the length of a thread span from the left edge of one primary droplet to the left edge of another primary droplet farther along the thread. We measured two or three thread spans per individual. To maximize the number of droplets included in the span we measured some *Araneus marmoreus*, *Argiope aurantia* and *Argiope trifasciata* threads under a dissecting microscope. The droplet distributions of other threads were determined from images made at low magnification under a compound microscope. For each individual spider we calculated DPMM as the total number of primary droplets included in the measured spans divided by the total span length and then computed the mean value for each species. The mean number of primary droplets included in a thread span ranged from 14 in *Argiope aurantia* to 27 in *Micrathena gracilis* to 54 in *Mangora maculata*. As thread stickiness was measured with contact plates of four widths, we computed the number of primary droplets that contacted each plate (PDPP) by multiplying DPMM by plate width (PWIDTH) expressed in mm.

We measured the length (dimension parallel to the thread's axial fibers) and width of three primary droplets (PL and PW, respectively) on two higher-magnification images of each spider's threads and the length and width of the secondary droplets, if any, included in these spans (SL, SW, respectively). We divided the total number of secondary droplets in a span by the total number of primary droplets to obtain the ratio of an individual's secondary to primary droplets (SPRATIO) and then computed mean values for individuals and species.

The outline of the lower half of a droplet is close to the shape of a parabola (Opell and Hendricks, 2007). Therefore, we computed the volume of each individual's primary and secondary droplets (PV and SV, respectively) as the volume of a parabola rotated around the *x*-axis using the following formulas:

$$PV = (2\pi\ PW^2\ PL)/15\ , \quad (1)$$

$$SV = (2\pi\ SW^2\ SL)/15\ . \quad (2)$$

Fig. 2 shows the relationship between DPMM and primary droplet volume. We also calculated an index that we term SHAPE from the mean PL and PW of each species as P in equation of a parabola defined by the outline of the lower half of a droplet: $Y=X^2/(2P)$, where X is PL/2 and Y is PW/2. Thus, $P=PL^2/(4PW)$. The larger the value of P, the more elongated the droplet along the axial fibers; the smaller the value of P, the more spherical the droplet.

We computed the total number of secondary droplets per contact plate (SDPP) as the product of PDPP and SPRATIO, and the total volume of secondary droplets per contact plate (SVPP) as the product of SDPP and SV.

We calculated the proportion of water in primary droplets because their larger size permitted us to measure their dimensions more accurately than those of secondary droplets and because they comprise the greatest amount of the thread's viscous material. At the time we collected thread samples for use in the measurements described above, we also collected thread samples from each individual's web on microscope slides with more widely spaced supports, also covered with double-sided tape on their upper surfaces. These we placed in microscope slide boxes and stored in a desiccating cabinet. Approximately 1 year later, we sputter-coated these threads with 50 nm of gold palladium and photographed them under the high vacuum of a scanning electron microscope (Fig. 3). We measured the droplets as above and computed the desiccated primary droplet dry volume (PDV) of each individual's threads using the formulas given above. We then calculated the volume of water in each individual's fresh primary droplets (PWV) as its PV–PDV and calculated the proportion of water in the primary droplets (PH2O) as PWV/PV.

In species whose threads had closely spaced primary and secondary droplets, we could not clearly delineate the boundaries of the primary and secondary droplets after these threads were flattened on cover slips. Therefore, we measured the total flattened

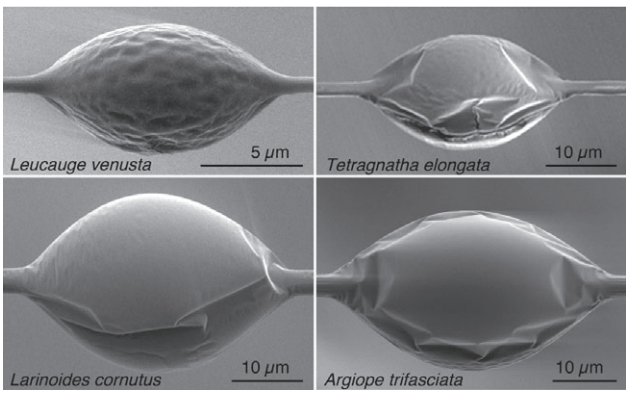

Fig. 3. Examples of desiccated viscous droplets.

droplet area of two threads from each individual's web and the lengths of these thread spans. We then divided the thread's surface area by its span length to obtain the surface area per millimeter (APMM). Multiplying APMM by PWIDTH in mm yields the surface area of primary and secondary droplets that contact a plate (APP). Flattening droplets also makes it possible to observe a thread's glycoprotein granules. We characterized granule shape, measured their dimensions and, from these data, determined their flattened surface areas and estimated their volumes.

Determining effective droplet number

Droplets at the edges of thread contact make the greatest contribution to thread stickiness and those at the center the least (Opell and Hendricks, 2007). This decreasing adhesive contribution of successive interior droplets should result in a droplet span beyond which no additional thread stickiness is registered. To account for this pattern of declining adhesion we used the same common denominator to compute an effective droplet number (EDN) for each species' threads on each of the four contact plate widths. EDN describes the total droplet equivalents that contribute to a thread's stickiness.

For this purpose we previously (Opell and Hendricks, 2007) used a common denominator of 2.0 to compute an approximate EDN. However, in this study we empirically determined which common denominator produced the 64 EDN values (one value for threads of each of the 16 species on each of the contact plates of four widths) used to model stickiness per contact plate. We did this by first computing 10 sets of 64 EDN values, one for each denominator from 1.1 to 2.0. After finding that the R^2 of the six-variable regression model described in the Results was greatest for EDN values computed with a common denominator of 1.4, we then computed sets of 64 EDN values for denominators 1.40 to 1.45. A comparison of the fit of these denominator values shows that a denominator of 1.43 produces the six-variable regression model with the greatest R^2 (Fig. 4). Therefore, we computed EDN such that each successively interior droplet contributed 1/1.43=0.6993 the adhesion of the next outermost droplet (Fig. 5).

Measuring residual extensibility of threads

We define the residual extensibility (RE) of a thread as the ratio of its length at rupture to its native, in-web length. This index is the same as breaking extension and describes the amount of extensibility

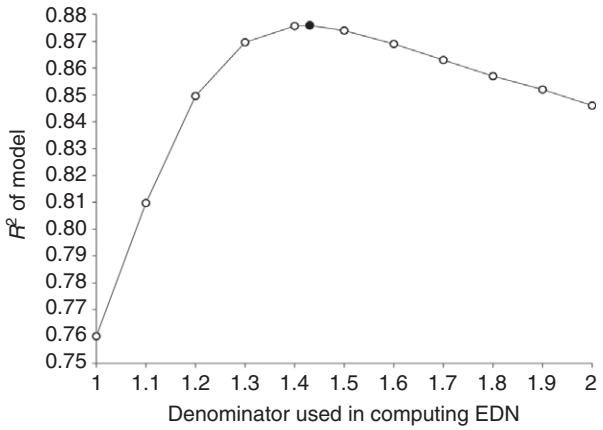

Fig. 4. Determination of the denominator used for computing effective droplet number (EDN). The corresponding R^2 values of these models reach a maximum value of 0.876 at a denominator of 1.43 (filled circle).

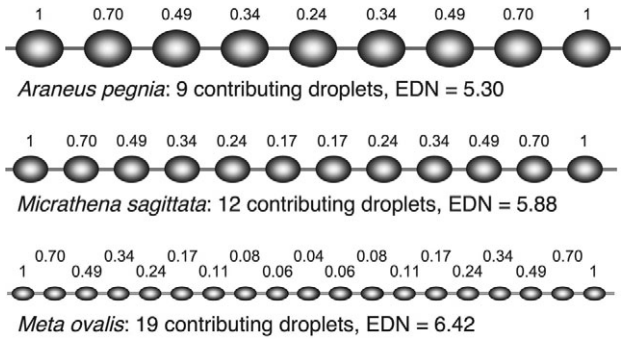

Fig. 5. Computation of the EDN of *Araneus pegnia* (8.6 droplets per millimeter, DPMM), *Micrathena sagittata* (11.4 DPMM) and *Meta ovalis* (20.6 DPMM) contacting 963 μm wide plates. Each interior droplet contributes 1/1.43=0.6993 the adhesion of the next outer droplet.

remaining in a viscous thread after a spider manipulates it during web construction. We measured RE by capturing viscous capture threads on 5 mm wide bars that were attached to the jaws of a digital caliper opened to a distance of 3 mm. Double-sided carbon tape (used for mounting specimens to be examined with a scanning electron microscope) secured threads to bars. Threads were then gently pressed into the tape with a smooth surface. To hold these threads even more securely, we applied Kores® mimeograph correction fluid (Ink Technology, Tenafly, NJ, USA) along the length of thread spans that contacted the tape. This red fluid is a fast-drying paint whose principal solvent appears to be ether. It did not wick onto suspended threads but immediately adhered to the double-sided tape and, when dry, formed a thin seal on the tape's surface. We then slowly separated the jaws of the caliper at a speed of approximately 232 μm s^{-1} until each of the strands broke. We computed the mean RE of at least 10 threads for most individuals and 4–11 individuals per species. Although we believe that the combined use of tape and mimeograph fluid held the threads securely, it is possible that the viscous material allowed some axial fiber slippage. However, RE exhibited an interspecific range of 3.53 to 9.06, indicating that this index is useful in characterizing the extensibility of threads at their native web tensions.

Thread extensibility and contact plate width effects

Differences in both the RE of a thread and the width of the contact plate used to measure thread stickiness have the potential to introduce artifacts into measurements of thread stickiness. As force increases, threads that are more extensible permit a contact plate to move further from the supports to which the thread is anchored before generating force and, in so doing, form a greater angle with the contact plate (Fig. 6, C *vs* B). Likewise, as the width of a contact plate increases and the lengths of suspended threads on either side of the contact plate decrease, these threads form a greater angle with the contact plate (Fig. 6, B *vs* A). As the angle between a thread and a contact plate increases, more force is directed perpendicular rather than parallel to the contact plate, causing the outer-most thread droplet to be pulled from the plate more easily and reducing the efficiency with which the adhesion of inner droplets is recruited. Consequently, greater RE and greater PWIDTH both have the potential to introduce negative artifacts into measured stickiness. We tested these hypothesized artifacts by determining whether RE, PWIDTH, or an interaction between RE and PWIDTH was related to stickiness.

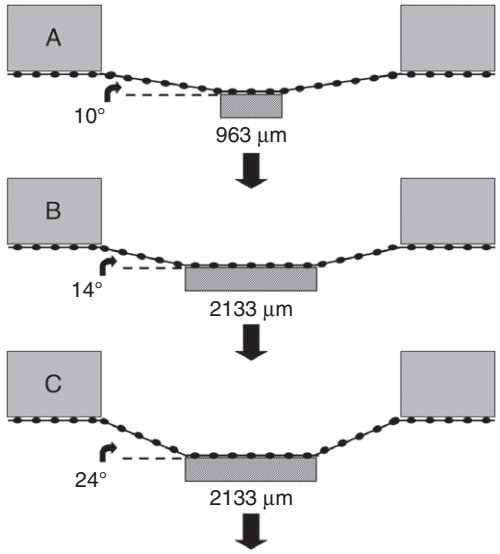

Fig. 6. An illustration of how increasing contact plate width (A to B) and an increase in thread elasticity (B to C) result in greater angles of contact between a thread and the edge of a contact plate, increasing the tendency for the thread to pull free of the plate.

Measuring thread stickiness

We measured the stickiness of 12 thread strands per web, three sectors with each of four contact plates having widths of 963, 1230, 1613 and 2133 μm. Prior to beginning each measurement, temperature and relative humidity were recorded. Our stickiness-measuring instrument incorporated a manipulator for aligning thread samples, a linear actuator for moving thread samples, and a load cell for recording the force of adhesion generated by threads. A thread was first pressed against the contact plate at a speed of $60\,\mu m\,s^{-1}$ until a force of 25 μN was generated and was then immediately withdrawn at the same speed until the thread pulled free of the contact plate. The maximum force registered by a thread was recorded as its stickiness. The mean value registered by each plate width was recorded as an individual's stickiness profile (stickiness per plate, SPP). We measured thread stickiness with a smooth acetate plate (Scotch® Magic™ Tape 810 Product Information Sheet, 2002; 3M) to maximize stickiness and to eliminate the possibility that threads with different droplet profiles might respond differently to a textured surface. We measured each thread with an unused region of the surface and renewed the acetate frequently.

Modeling thread stickiness

We used the Statistical Analysis System (SAS Institute, Cary, NC, USA) to construct a regression model showing the relationships of the following six independent variables to thread stickiness, accepting as significant $P \leq 0.05$. We examined other variables in addition to those listed below, but excluded them after finding that they were not significant or were correlated with one another or the six retained variables for obvious functional or compositional reasons. After constructing the six-variable model we examined each variable's proportional contribution to stickiness to determine whether there were groups of species in which a particular variable made an unusually high or low contribution, as might be expected if there are different ways to optimize thread stickiness.

EDN: effective droplet number on a given plate width.

SHAPE: twice the focal length of the parabola defined by the outline of the lower half of a primary droplet. As SHAPE is computed from droplet length and width, these variables were not included in the model.

SVPP: secondary droplet volume per contact plate.

PH2O: the proportion of water in primary droplets.

APP: the surface area of flattened primary and secondary droplets contacting a plate.

RE: residual extensibility (equivalent to breaking extension).

The failure of glycoprotein granules to contribute to the model

Those familiar with viscous threads may find the absence of glycoprotein granule features from this list of model variables surprising. These granules form within thread droplets soon after they coalesce and are thought to be largely responsible for the thread's adhesion (e.g. Vollrath and Tillinghast, 1991; Tillinghast et al., 1993). However, each of our attempts to find a relationship between any granule feature and thread stickiness either failed or showed a small, negative contribution of granule size to thread stickiness. Therefore, as the granule data set and the images required to document it are extensive, we present these data in a separate study.

RESULTS

Tables 1 and 2 describe the features of the 16 species' threads. Spider mass exhibits an inverse, allometric relationship to the number of droplets per millimeter (DPMM=38.85–5.5834 ln mass; P=0.0169, R^2=0.34) and a direct, isometric relationship to primary droplet volume (PV=78.3823 mass+1916.44; P=0.0001, R^2=0.68). This is reflected in an allometric decline in both primary droplet volume and the volume of primary droplets per millimeter thread length as the number of droplets per millimeter increases (Fig. 2).

Using EDN it is possible to estimate the number of droplets in a thread span beyond which little or no additional stickiness accrues, a value that we (Opell and Hendricks, 2007) have termed 'maximum efficiency span', as the number of contacting droplets beyond which EDN shows no appreciable increase. Fig. 7 shows this value to be in the range of 20 droplets.

Correlations among the model variables are shown in Table 3. For each plate width RE was negatively, but insignificantly, correlated with SPP (963 μm: –0.34, P=0.20; 1230 μm: –0.29, P=0.27; 1613 μm: –0.24, P=0.38; and 2133 μm: –0.26, P=0.33). When all plate widths were included RE was negatively and significantly related to SPP (P=0.0141), although neither PWIDTH nor the interaction between RE and PWIDTH was significant (P=0.1958 and 0.1221, respectively). Consequently, there is evidence for an RE negative artifact, but no support for a PWIDTH artifact.

Figs 8–10 show the mean stickiness values that threads of the 16 study species registered on contact plates of 963, 1230, 1613 and 2133 μm width. When included in a regression model, each of the six variables described above had P=0.0001 except RE, which had P=0.0019. Together these variables constitute the following regression model that describes thread stickiness per plate (SPP) and has P=0.0001 and R^2=0.88:

$$SPP = (62.2537EDN) + (15.0522SHAPE) + (0.0020SVPP) - (213.6091PH2O) - (11.4523RE) - (0.0006APP) - 202.3569 . \quad (3)$$

A maximum R^2 improvement analysis added these values in the following order as it increased the model's fitness: PH2O (R^2=0.42),

Table 2. Computed features of viscous threads

Species	*N*	Primary droplet volume (μm^3)	Secondary droplet volume (μm^3)	Secondary to primary droplet ratio	Primary droplet shape (μm)	Proportion of water	Flattened droplet area ($\mu m^2\ mm^{-2}$)	Residual extensibility
Argiope aurantia	5	59287±11404	1073±364	1.14±0.19	24.45	0.49±0.03 (3)	63363±11385	6.33±0.49
Araneus marmoreus	10	79730±13708	3264±725 (7)	0.69±0.15	22.44	0.48±0.11 (4)	128561±15379	6.53±0.62
Argiope trifasciata	11	12005±2150	1314±263	1.41±0.29	17.15	0.41±0.15 (3)	30834±2747	6.41±0.68
Araneus bicentenarius	6	43234±13694	2353±1017	0.79±0.12	15.33	0.63±0.12 (3)	63117±8216	9.06±1.06
Larinioides cornutus	4	20264±9409	12021±6994	0.58±0.14	14.13	0.29±0.08 (4)	34513±1935	3.97±0.50
Verrucosa arenata	5	6055 ±694	243±162 (4)	0.33±0.18	8.65	0.39±0.06 (3)	27084±5456	3.53±0.33
Araneus pegnia	9	15124±3656	1340±1176 (3)	0.08±0.04	13.15	0.66±0.05 (5)	120726±5554 (7)	6.74±0.82
Micrathena gracilis	5	7510±1510	453±129 (4)	0.65±0.20	9.71	0.43±0.09 (4)	100813±38605	8.69±0.60
Theridiosoma gemmosum	5	1249±746	387±284	0.81±0.39	4.49	0.53±0.15 (2)	8743±2332	3.82±0.34
Micrathena sagittata	5	4622±766	286±135	0.72±0.13	8.37	0.32±0.11 (4)	131080±9793	5.39±0.18
Tetragnatha elongata	4	5846±2332	161±113 (3)	0.60±0.25	9.93	0.03±0.02 (3)	26665±8293	5.13±0.98
Metepeira labyrinthea	8	3014±632	203±124	1.05±0.21	8.42	0.66±0.07 (4)	31117±3946	6.89±0.64
Meta ovalis	8	896±146	37±16	0.39±0.09	4.68	0.57±0.08 (5)	12989±2071 (7)	4.53±0.27
Leucauge venusta	10	698±186	39±7 (7)	0.35±0.11	4.74	0.70±0.08 (5)	15105±2314 (8)	4.98±0.19
Cyclosa turbinata	9	608±149	74±10	0.85±0.07	4.43	0.57±0.18 (4)	19679±4114 (8)	5.63±0.38
Mangora maculata	6	40±7	13±3 (4)	0.29±0.14	1.09	0.68±0.06 (5)	390±222	4.93±0.28

Means ± 1 s.e. Numbers in parentheses give the sample size if less than that listed in the second column.

SVPP (R^2=0.64), APP (R^2=0.68), SHAPE (R^2=0.75), EDN (R^2=0.85), RE (R^2=0.88).

Although the modeled and measured stickiness correspond well overall (Figs 8–10) the values of *Araneus marmoreus*, *Araneus pegnia*, *Micrathena gracilis*, *Theridiosoma gemmosum*, *Micrathena sagittata* and *Cyclosa turbinata* differed conspicuously from their modeled values. When modeling the proportional contribution of the model's six variables according to the above composite model (Fig. 11, composite model), we identified three groups of species in which a particular variable made an unusually high or low contribution to modeled stickiness. The regression model of each of these three groups had P=0.0001 and a higher R^2 value than the composite 16 species model. Consequently, their modeled stickiness values were consistently more similar to measured stickiness than were their values under the composite model (Figs 8–10).

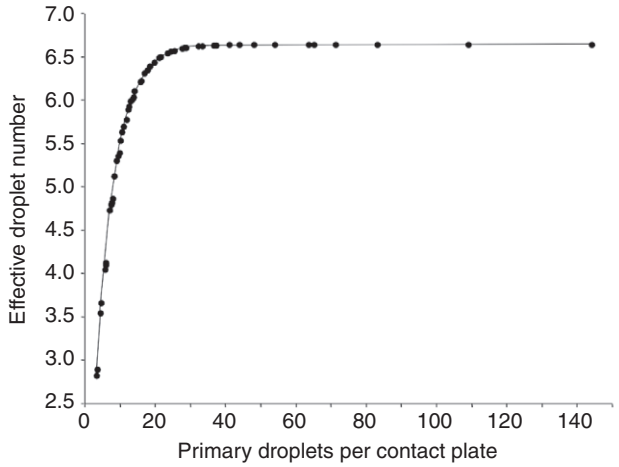

Fig. 7. Relationship between the number of primary droplets that contact a plate and effective droplet number (EDN), showing that there is little increase in EDN, and, therefore, thread stickiness, beyond a value of 20 droplets.

Group 1 included *Argiope aurantia*, *Araneus bicentenarius*, *Argiope trifasciata*, *Larinioides cornutus*, *Leucauge venusta*, *Metepeira labyrinthea*, *Tetragnatha elongata* and *Verrucosa arenata*, which in the composite model were characterized by large APP and SHAPE contributions. In this model all variables

Table 3. Correlations among the variables used to model thread stickiness

	SHAPE	SVPP	PH2O	APP	RE
EDN					
Composite	–0.84**	–0.24	0.16	–0.21	–0.22
Group 1	–0.80**	–0.11	0.06	–	–0.15
Group 2	–0.86**	–0.59*	–0.15	0.33	–
Group 3	–0.30	–0.34	0.51*	0.23	0.66*
SHAPE					
Composite		0.34*	–0.22	0.48**	0.41**
Group 1		0.22	–0.10	–	0.36*
Group 2		0.79**	0.34	0.11	–
Group 3		0.46	–0.94**	0.69*	–1.20
SVPP					
Composite			–0.29*	0.07	–0.13
Group 1			–0.23	–	–0.23
Group 2			–0.14	0.38	–
Group 3			–0.66	0.38	–0.32
PH2O					
Composite				–0.10	0.24
Group 1				–	0.48*
Group 2				–0.04	–
Group 3				–0.54*	0.42
APP					
Composite					0.47**
Group 1					–
Group 2					–
Group 3					0.38

SHAPE, twice the focal length of the parabola defined by the outline of the lower half of a primary droplet; EDN, effective droplet number; SVPP, total volume of secondary droplets per contact plate; PH2O, proportion of water in the primary droplets; APP, surface area of primary and secondary droplets that contact a plate; RE, residual extensibility.
*0.0007<P≤0.05. **P≤0.0007.

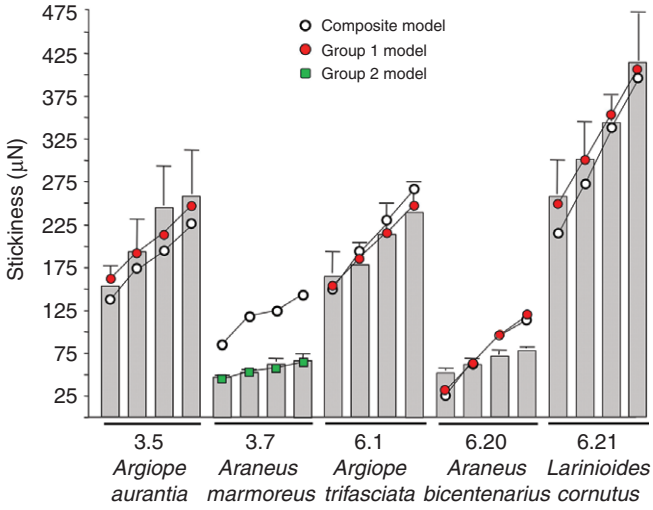

Fig. 8. Histogram of mean stickiness registered on plates of 963, 1230, 1613 and 2133 µm width by the five species with the fewest primary droplets per millimeter, as shown above the species name. Error bars represent ±1 s.e. Symbols connected by lines show modeled values.

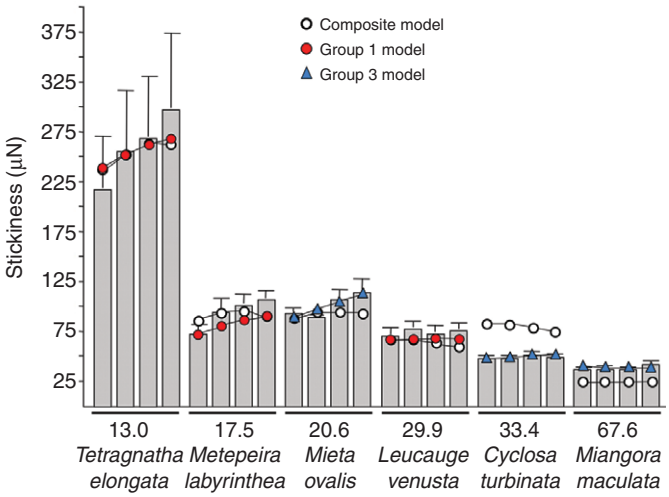

Fig. 10. Histogram of mean stickiness values registered on plates of 963, 1230, 1613 and 2133 µm width by the six species with the greatest number of primary droplets per millimeter, as shown above the species name. Error bars represent ±1 s.e. Symbols connected by lines show modeled values.

contributed at P=0.0001, except APP, which, with P=0.0974, was excluded from the model. The model, as described below, had R^2=0.97:

$$\text{SPP} = (39.0259\text{EDN}) + (11.1388\text{SHAPE}) + (0.0019\text{SVPP}) - (216.1721\text{PH2O}) - (19.2173\text{RE}) + 0.5515 . \quad (4)$$

A maximum R^2 improvement analysis added these values in the following order as it increased the model's fitness: PH2O (R^2=0.60), SVPP (R^2=0.85), SHAPE (R^2=0.88), EDN (R^2=0.91), RE (R^2=0.97).

Group 2 included *Araneus marmoreus*, *Araneus pegnia*, *Micrathena gracilis* and *Micrathena sagittata*, which in the composite model were characterized by a small APP contribution. This model retained EDN, SHAPE, SVPP and APP (P<0.0014), but excluded PH2O and RE (P>0.62) and had R^2=0.96. The contribution of SVPP changed from positive to negative and the contribution of APP changed from negative to positive (Fig. 11).

$$\text{SPP} = (14.5445\text{EDN}) + (3.9462\text{SHAPE}) - (0.0027\text{SVPP}) + (0.0001\text{APP}) - 78.1351 . \quad (5)$$

A maximum R^2 improvement analysis added these values in the following order as it increased the model's fitness: APP (R^2=0.46), SVPP (R^2=0.75), SHAPE (R^2=0.88), EDN (R^2=0.96).

Group 3 included *Cyclosa turbinata*, *Mangora maculata*, *Meta ovalis* and *Theridiosoma gemmosum*, which in the composite model were characterized by a small SHAPE contribution. This model retained all variables (P<0.0021) except PH2O (P<0.2511) and had

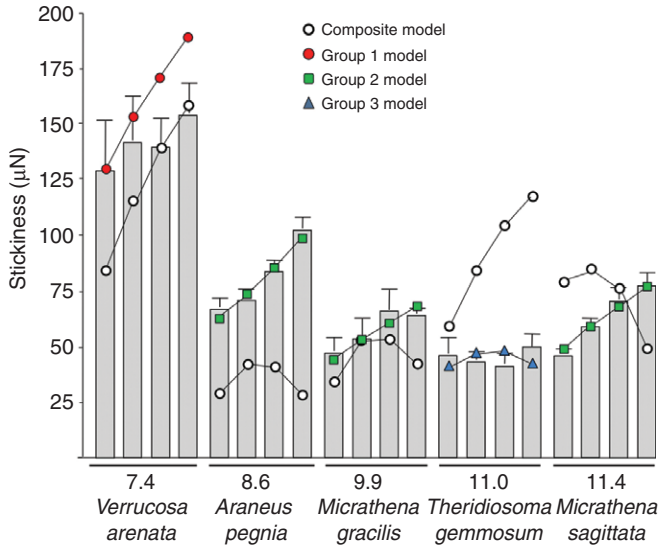

Fig. 9. Histogram of mean stickiness values registered on plates of 963, 1230, 1613 and 2133 µm width by the five species with intermediate numbers of primary droplets per millimeter, as shown above the species name. Error bars represent ±1 s.e. Symbols connected by lines show modeled values.

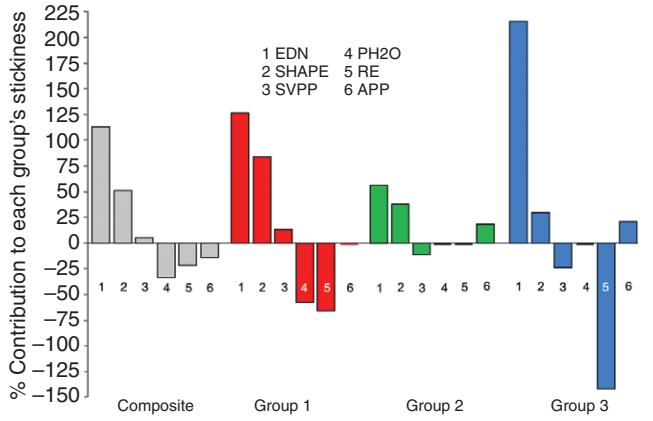

Fig. 11. Contributions of the six components of the regression model that describes the stickiness expressed by viscous thread on contact plates of four widths for the composite model and for group 1, 2 and 3 models. SHAPE, twice the focal length of the parabola defined by the outline of the lower half of a primary droplet; SVPP, total volume of secondary droplets per contact plate; PH2O, proportion of water in the primary droplets; RE, residual extensibility; APP, surface area of primary and secondary droplets that contact a plate.

R^2=0.97. As in the group 2 model the contribution of SVPP changed from positive to negative and the contribution of APP changed from negative to positive (Fig. 11).

$$SPP = (34.4850EDN) + (8.1900SHAPE) - (0.0121SVPP) + (698.8896PH2O) - (31.0785RE) + (0.0013APP) - 46.0925 . \quad (6)$$

A maximum R^2 improvement analysis added these values in the following order as it increased the model's fitness: SHAPE (R^2=0.25), SVPP (R^2=0.72), RE (R^2=0.77), APP (R^2=0.89), EDN (R^2=0.92), SHAPE (R^2=0.97).

DISCUSSION

These results confirm the observation that capture threads register increased stickiness when measured with contact plates of increasing width (Figs 8–10) (Opell and Hendricks, 2007). However, with the exception of *Theridiosoma gemmosum*, this progression is restricted to threads of the 13 species having 20 or fewer DPMM. This assessment corresponds with an empirical examination of the rate of EDN increase with increasing DPMM, which also suggests that beyond a thread span composed of 20 droplets, little additional stickiness accrues (Fig. 7). This value is greater than the 'maximum efficiency span' of 12 droplets we estimated previously (Opell and Hendricks, 2007) because in the current study we used an empirically determined common denominator of 1.43 rather than an estimated value of 2.0 to compute EDN. Stickiness does not increase in proportion to plate width because of the declining increase in EDN as droplet number increases (Fig. 5).

In all models EDN makes the greatest positive contribution to stickiness, followed by SHAPE (Fig. 11), indicating that, for most species, the total effective amount of viscous material that contacts a surface is the greatest determinant of thread stickiness. For droplets of a given volume, SHAPE increases as droplets elongate along axial fibers. Consequently, other features being equal, droplets that are more viscous should have larger SHAPE values. SVPP makes either the smallest positive or the smallest negative contribution to stickiness. Although it is difficult to understand why this variable would reduce stickiness, its small contribution is easily explained by the small size of secondary droplets.

A positive correlation between APP and PH2O might be expected, as droplets with a higher proportion of water should be less viscous and, therefore, flatten to a larger area. However, the only correlation between APP and PH2O is a negative one seen in group 3 species (Table 2), suggesting that droplet viscosity is not dependent on droplet water content. PH2O makes either no contribution or a large negative contribution to stickiness, indicating that droplets with a higher percentage of water have a lower concentration of chemicals that contribute to adhesion. In the comprehensive model, APP makes a small negative contribution to stickiness, although it either fails to contribute to the group models or makes a small positive contribution to stickiness.

RE has either no effect or a negative effect on stickiness, supporting the hypothesis that more elastic threads form greater edge angles of contact with plates, reducing their ability to recruit adhesion from interior droplets and making it easier for them to be pulled from a contact plate. The negative impact of RE is most strongly expressed in group 3, where the small number of species results in a contrast between the low measured RE of *Theridiosoma gemmosum* and the higher values of the other three species. We found no evidence that PWIDTH imposed an artifact on the measurement of thread stickiness.

The issue of measurement artifact bears on our recent study of axial fiber extensibility and viscous thread stickiness (Opell et al., 2008). This study showed that thread extensibility contributes to thread stickiness by facilitating the recruitment of adhesion from multiple viscous droplets. By stretching threads to reduce their extensibility and then measuring the stickiness of these threads with contact plates whose widths increased proportionately to thread elongation, the study maintained the number of droplets contributing to stickiness as the thread's extensibility decreased. The current study indicates that thread elongation also reduced the edge angles of contact between threads and contact plates (Fig. 6, B *vs* C), thereby slightly reducing their stickiness. Consequently, in the 2008 study it was only possible to document the positive contribution of thread extensibility to thread stickiness because this contribution overcame the negative artifact documented in the current study. Our inability to detect a measurement artifact of PWIDTH also meant we failed to call into question the conclusions of the previous study.

We attempted to measure and characterize all of the features of capture threads that our instrumentation would permit. However, other features such as the chemical composition of the viscous material and the Young's modulus of the axial fiber may affect thread stickiness. Our effort to standardize the humidity under which threads were photographed and their stickiness measured probably resulted in the threads of some species being measured under a humidity different from that of their typical habitats. We do not know whether the concentration or strength of hydrophilic compounds in viscous droplets differs among species or, if they do, whether droplets from dry or moist habitats are more hydrophilic. When we divide the species we studied into putative high humidity (HH) and low humidity (LH) habitat groups (HH: *Araneus bicentenarius*, *Leucauge venusta*, *Mangora maculata*, *Meta ovalis*, *Micrathena gracilis*, *Micrathena sagittata*, *Tetragnatha elongata*, *Theridiosoma gemmosum* and *Verrucosa arenata*; LH: *Argiope aurantia*, *Araneus marmoreus*, *Araneus pegnia*, *Argiope trifasciata*, *Cyclosa turbinata*, *Larinioides cornutus and Metepeira labyrinthea*) there was no difference in either the humidity under which threads were photographed (mean ± s.e., HH 50.7±1.2%, LH 47.5±3.3%; *t*-test P=0.39) or the proportion of water in their droplets (mean ± s.e., HH 0.48±0.07, LH 0.51±0.05; *t*-test P=0.73). Consequently, differences between environmental and laboratory humidity do not appear to have imposed a systematic bias on our results.

Our results show that there is no single scaling factor that explains the range of features observed in viscous threads and that similar adhesion can be achieved by threads with quite different combinations of features, even among species in the same model group. This is seen clearly when features of the two stickiest threads, those produced by *Larinoides cornutus* and *Tetragnatha elongata*, both in group 1, are compared (Figs 8 and 10). Threads of *Tetragnatha elongata* have primary and secondary droplet volumes that are only 30% and 1%, respectively, those of *Larinoides cornutus* (Table 2). However, two other variables compensate for this difference in droplet size. With twice the droplets per millimeter, *Tetragnatha elongata* has a greater effective droplet number (5.934 for a 963 μm wide contact plate, compared with 4.125 for *Larinoides cornutus*) and, with only 3% water content, little stickiness is lost to this variable. The more pronounced increase in stickiness that *Larinoides cornutus* threads register on contact plates of increasing width is explained by their smaller number of droplets per millimeter and an associated larger increase in EDN. With only 6.21 droplets per millimeter, the EDN of *Larinoides cornutus* threads show a 46% increase from the narrowest to the widest plate; whereas with 13.0 droplets per millimeter, *Tetragnatha elongata* threads show only an 11% increase.

However, droplet number alone is not a good predictor of stickiness. *Araneus bicentenarius*, also in group 1, has the same

number of droplets per millimeter and the same EDN as *Larinoides cornutus*, but its threads exhibit only one-quarter the stickiness (Fig. 8), even though its primary and secondary droplets have twice the volume of those of *Larinoides cornutus* (Table 2). The low stickiness of *Araneus bicentenarius* threads can be attributed to two factors: (1) a residual extensibility that is more than twice that of *Larinoides cornutus* and (2) primary droplets with twice the water content of *Larinoides cornutus*.

Within the context of droplet sizes, which tend to be directly related to spider size, and droplet spacing, which tends to be inversely related to spider size, two hypotheses may account for the combinations and range of features seen in the threads of the 16 species that we studied. Thread features may be selected to optimize thread performance in the context of a particular habitat, web architecture or prey type. Alternatively, thread features may be shaped largely by other factors, such as a species' phylogenetic history or the metabolic cost or efficiency of producing thread components. A test of these hypotheses could come from comparison of pairs of similarly sized congeners that occupy similar and dissimilar habitats.

Although our data are not sufficient for a comprehensive test, the three qualifying species pairs that they do contain provide tentative support for a habitat effect on thread features. Members of the *Argiope aurantia–Argiope trifasciata* (group 1 model) and of the *Micrathena gracilis–Micrathena sagittata* (group 2 model) species pairs are found in the same habitats, sometimes with webs less than a meter apart. The *Argiope* species pair inhabits exposed weedy areas and the *Micrathena* species pair inhabits moist forests. The members of each group have similar stickiness values and, when body size-related differences in droplet size and spacing are taken into account, each member has similar thread features. In contrast, members of the third species pair live in different habitats and are characterized by different group models. *Araneus marmoreus* (group 2) has a holarctic distribution and is a common inhabitant of trees and shrubs of the forest edge (Levi, 1971), whereas in our region *Araneus bicentenarius* (group 1) appears restricted to moist, high elevation forests of the Appalachian Mountains (Levi, 1971). Although the threads of these two species have similar stickiness (Fig. 8), their values are described by different models, which assign different weights to their thread features (Fig. 11), indicating that different selective factors have shaped their thread features. A potential problem with this preliminary analysis is that, in the absence of phylogenetic studies, it assumes a similar degree of relatedness of the members of each species pair.

Our findings on the positive contributions to stickiness by both effective droplet number and the size and shape of primary viscous droplets, and the negative artifact of axial fiber residual extensibility appear to apply to most viscous threads. The role of other features, such as the small positive contribution to stickiness made by secondary droplets and the negative contributions of both the proportion of water in viscous droplets and the flattened area of threads may apply to many but not all threads. A fuller understanding of interspecific differences in the chemical composition of viscous droplets, in the performance characteristics of individual droplets, and in the mechanical properties of the thread's axial fibers may be necessary for a better understanding of the adhesive delivery system of viscous threads.

During this 3 year study Andrea Burger, Brian Segal, Mike Leonard, Lindsay Neist, Harry Schwend, Brian Markley, Chip Hannum, Genine Lipkey, Kaitlin Flora and Steve Vito helped collect, photograph and measure threads. National Science Foundation grant IOB-0445137 supported this research.

LIST OF ABBREVIATIONS

APMM	surface area per millimeter of flattened primary and secondary droplets
APP	surface area of flattened droplets on a contact plate of given width
DPMM	number of primary droplets per millimeter thread length
EDN	the total droplet equivalents that contribute to a thread's stickiness on a contact plate
PDPP	primary droplets per contact plate
PDV	desiccated volume of a primary droplet
PL	length of a primary droplet
PH2O	proportion of water in a primary droplet
PV	volume of a primary droplet
PW	width of a primary droplet
PWIDTH	contact plate width
PWV	volume of water in a primary droplet
RE	residual extensibility of a thread
SDPP	secondary droplets per contact plate
SHAPE	twice the focal length of a parabola defined by the lower half of a primary droplet
SL	length of a secondary droplet
SPP	stickiness per plate
SPRATIO	ratio of the number of secondary to primary droplets
SV	volume of a secondary droplet
SVPP	secondary droplet volume per contact plate
SW	width of a secondary droplet

REFERENCES

Agnarsson, I. and Blackledge, T. A. (2009). Can a spider web be too sticky? Tensile mechanics constrains the evolution of capture spiral stickiness in orb weaving spiders. *J. Zool.* **278**, 134-140.

Agnarsson, I., Boutry, C. and Blackledge, T. A. (2008). Spider silk aging: initial improvement in a high performance material followed by slow degradation. *J. Exp. Zool. Part A Ecol. Genet. Physiol.* **309A**, 494-504.

Blackledge, T. A. and Eliason, C. M. (2007). Functionally independent components of prey capture are architecturally constraigned in spider orb webs. *Biol. Lett.* **3**, 456-458.

Chacón, P. and Eberhard, W. G. (1980). Factors affecting numbers and kinds of prey caught in artificial spider webs with considerations of how orb-webs trap prey. *Bull. Br. Arachnol. Soc.* **5**, 29-38.

Coddington, J. A. and Levi, H. W. (1991). Systematics and evolution of spiders (Araneae). *Annu. Rev. Ecol. Syst.* **22**, 565-592.

Eberhard, W. G. and Pereira, F. (1993). Ultrastructure of cribellate silk of nine species in eight families and possible taxonomic implications. (Araneae: Amaurobiidae, Deinopidae, Desidae, Dictynidae, Filistatidae, Hypochilidae, Stiphidiidae, Tengellidae). *J. Arachnol.* **21**, 161-174.

Griswold, C. E., Coddington, J. A., Hormiga, G. and Scharff, N. (1998). Phylogeny of the orb-web building spiders (Araneae, Orbiculariae: Deinopoidea, Araneoidea). *Zool. J. Linn. Soc.* **123**, 1-99.

Griswold, C. E., Ramírez, M. J., Coddington, J. A. and Platnick, N. I. (2005). Atlas of phylogenetic data for eneelegyne spiders (Araneae: Araneomorphae: Entelegynae) with comments on their phylogeny. *Proceedings Calif. Acad. Sci.* **56,** Suppl. 2, 1-324.

Levi, H. W. (1971). The *Diadematus* group of the orb-weaver genus *Araneus* North of Mexico (Araneae: Araneidae). *Bull. Mus. Comp. Zool.* **141**, 131-179.

Opell, B. D. (1994). Factors governing the stickiness of cribellar prey capture threads in the spider family Uloboridae. *J. Morphol.* **221**, 111-119.

Opell, B. D. (1999). Changes in spinning anatomy and thread stickiness associated with the origin of orb-weaving spiders. *Biol. J. Linn. Soc.* **68**, 593-612.

Opell, B. D. and Hendricks, M. L. (2007). Adhesive recruitment by the viscous capture threads of araneoid orb-weaving spiders. *J. Exp. Biol.* **210**, 553-560.

Opell, B. D. and Schwend, H. S. (2008a). Adhesive efficiency of spider prey capture threads. *Zoology* **112**, 16-26.

Opell, B. D. and Schwend, H. S. (2008b). Persistent stickiness of viscous capture threads produced by araneoid orb-weaving spiders. *J. Exp. Zool.* **307A**, 11-16.

Opell, B. D., Markley, B. J., Hannum, C. D. and Hendricks, M. L. (2008). The contribution of axial fiber extensibility to the adhesion of viscous capture threads spun by orb-weaving spiders. *J. Exp. Biol.* **211**, 2243-2251.

Peters, H. M. (1984). The spinning apparatus of Uloboridae in relation to the structure and construction of capture threads (Arachnida, Araneida). *Zoomorphology* **104**, 96-104.

Peters, H. M. (1986). Fine structure and function of capture threads. In *Ecophysiology of Spiders* (ed. W. Nentwig), pp. 187-202. New York: Springer-Verlag.

Peters, H. M. (1992). On the spinning apparatus and structure of the capture threads of Deinopis subrufus (Araneae, Deinopidae). *Zoomorphology* **112**, 27-37.

Tillinghast, E. K., Townley, M. A., Wight, T. N., Uhlenbruck, G. and Janssen, E. (1993). The adhesive glycoprotein of the orb web of *Argiope aurantia* (Araneae, Araneidae). *Mater. Res. Soc. Symp. Proc.* **292**, 9-23.

Townley, M. A., Bernstein, D. T., Gallanger, K. S. and Tillinghast, E. K. (1991). Comparative study of orb-web hydroscopicity and adhesive spiral composition in three areneid spiders. *J. Exp. Zool.* **259**, 154-165.

Vollrath, F. (1992). Spider webs and silks. *Sci. Am.* **266**, 70-76.

Vollrath, F. and Tillinghast, E. K. (1991). Glycoprotein glue beneath a spider web's aqueous coat. *Naturwissenschaften* **78**, 557-559.

Vollrath, F., Fairbrother, W. J., Williams, R. J. P., Tillinghast, E. K., Bernstein, D. T., Gallagher, K. S. and Townley, M. A. (1990). Compounds in the droplets of the orb spider's viscid spiral. *Nature* **345**, 526-528.